North Asian International Research Journal of Sciences, Engineering & I.T.

ISSN: 2454-7514 Vol. 11, Issue-7, July-2025

IRJIF. I.F. : 3.821

Index Copernicus Value: 52.88 Indian Citation Index Thomson Reuters ID: S-8304-2016

NAIRJC UGC-Aligned | HEI-Approved Peer Reviewed Refereed Journal (Under New UGC Guidelines)

DOI: doiglobal.org/10.2025/NAIRJCPMS.048

JUDD-OFELT ANALYSIS OF ER^{3+} DOPED DIBORATE GLASSES USING UV-VISIBLE SPECTRA

G. CHANDRASHEKARAIAH[1], A. JAYASHEELAN[2], K.C. SURESH[3], J. SHIVAKUMAR[4],

[1]Department of Physics, Government First Grade College, Gubbi, Tumkur-572216, India

[2]Department of Physics, Maharani Science College for Women, Bangalore-560001, India.

[3]Department of Physics, Government First Grade College foe Women, Tumkur-572101, India

[4]Department of Physics, School of Engineering, Presidency University, Bangalore-560064, India

Government First Grade College, Kunigal, Tumkur-572130, India

(Correspondingauthor Email: shivakumarj225@gmail.com,)

1. INTRODUCTION

White light emitting diodes (WLED's) play a significant role in the development of next generation solid state illuminating devices due to their reliability, energy efficiency and luminous efficiency [1-4]. The white LED's commercially available are coated with phosphor containing rare earth (RE^{3+}) oxides [5-7] have poor color reproducibility, low thermal stability, low color rendering index and poor chemical durability [7]. Optical properties of RE^{3+} doped glassy materials play a pivotal role in laser technology as optical fibers, wave guides, amplifiers, IR-visible up converters and so on [8]. By modifying the covalency and local structure, optical properties can be tailored [9]. The rare-earth,Er^{3+}, doped glasses play a significant role in the development of lasers, optical amplifiers etc. [10]. The Bi_2O_3 is a conditional glass former, but it readily forms glass in combination with archetypal glass formers such asB_2O_3, Si_2O_3, P_2O_5, Ge_2O_3etc. [11]. The addition of glass formers increases the melting temperature and thermal stability of glass [12], while the addition of halides reduces the phonon energy and increases the transparency of glass [13,14]. It is important to study two photon absorption coefficient (TPA or β_2) which has application such as optical limiting [15], pumping lasing [16] and 3D optical data storage [4].On the other hand,β_2 can provide information about the micro-transparent flaws in the glass which can cause problems in the UV-Lasers.

B_2O_3 consists of planar $[BO_{3/2}]^0 (\equiv B_3)$ triangles with $B-O-B$angle lying between 120° and130°[[20,21].The addition of alkali oxides in the B_2O_3network ($[BO_{4/2}]^- \equiv B_4$units)$\left(\text{upto } \frac{\text{Alkali oxides}}{B_2O_3} = 0.35\right)$ and thus, the dimensionality and network connectivity can be enhanced. The quantification of $B_4$and B_4/B_3 ratio is important in assigning structural origin for the trends in physical properties. The study of structure of glass

can be made using Raman and infrared spectroscopy [22, 23]. The infrared spectra of single alkali diborate glasses can be used to estimate the amount of B_4 units and the normalized absorption area can be used to confirm the boron-oxygen tetrahedral structure. Theconcentration of B_4 estimated from the mid-IR spectra scales linearly with the fraction of B_4 atoms determined from the NMR study[24]. The aim of the proposed study is$Li_2B_4O_7$ base glass doped with $BiCl_3$ and$Er_2O_3$is (i) to calculate the J-O parameter and oscillatory strengths from the absorption spectra and refractive index, (ii) to analyze the luminescence characteristics of the coupled transitions $^2H_{11/2}+ {}^4S_{3/2}\rightarrow {}^4I_{15/2}$in the visible region, (iii) to evaluate the covalent/ionic nature of the investigated glasses and (iv) to identify different vibrational modes of linkages present in the network structure.

2. EXPERIMENTAL

The glass system with chemical compositions $90\ Li_2B_4O_7 + x\ Er_2O_3 + (10 - x)\ BiCl_3$(LBE) where $0.1 \leq x \leq 0.5$ was prepared by melt quenching method. Analar-gradeLi_2CO_3, $H_3BO_3$and $BiCl_3$were weighed in accordance with the above formula. Detailed account of the synthesis was described in our recent publication [12].

3. RESULT AND DISCUSSION

3.1 Judd-Ofelt intensity analysis

The Judd-Ofelt theory gives precise analogy of the intensity and accurate measurements of rare earth ions concentrations in the solids. The room temperature absorption spectra of LBE5 glass sample was recorded in the wavelength range of 400-800 nm as shown in Fig. 1 and Fig. 2and several peaks have been identified. These observed absorption peaks are incorporated with literature of the Er^{3+}doped various other glasses. The strong absorption peaks correspond to the transitions between various excited higher and the ground level [25-27]. The active absorption of the glass sample in ultraviolet range, the peaks below 420 nm [28]. The transitions from ground state to the excited states of pronouncedpeaks at 293, 301, 314, 355, 364, 377, 406, 441, 450, 488, 520 and 621 nm corresponding to $^4I_{15/2}\rightarrow {}^4G_{7/2}$, $^4G_{5/2}$, $^2P_{3/2}$, $^2G_{7/2}$, $^2K_{15/2}$, $^4G_{11/2}$, $^2G_{9/2}$, $^4F_{3/2}$, $^4F_{5/2}$, $^4F_{7/2}$, $^2H_{11/2}$, and $^4F_{9/2}$transitions respectively [29,30].

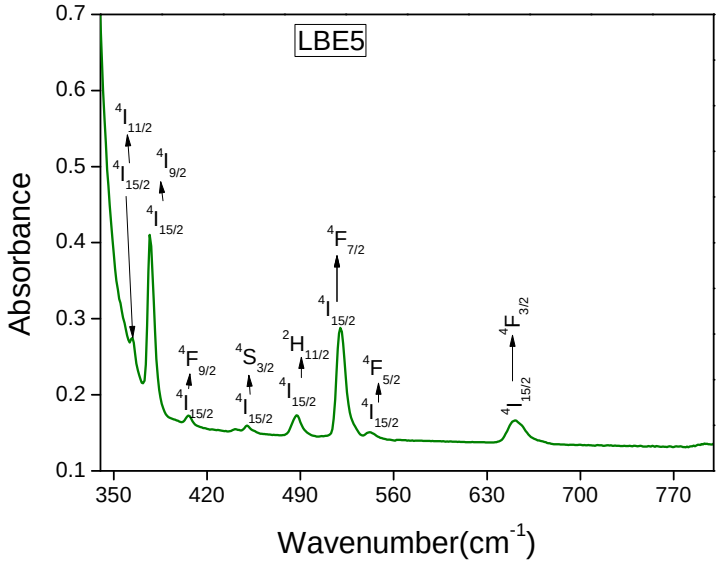


Fig 1. Optical absorbance of LBE5 and inset LB (without Er^{3+}) glass sample.

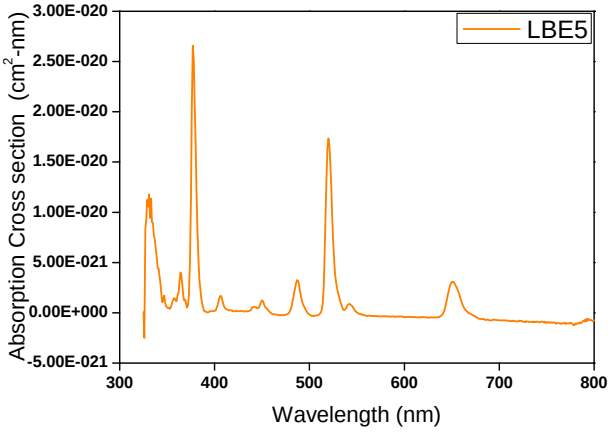


Fig 2. Room temperature absorption spectrum 0.5mol % of Er^{3+} doped LBE5 glass

The absorption coefficients (σ) were calculated [25,26] using the formula $\sigma = \frac{2.303\,A}{Nt}$, where A is the absorbance, N is the concentration of Er^{3+}ions, t is the thickness of the sample. The line strength was calculated using the formula [30]. The integrated absorption cross sectional areawas determined from the absorption spectra. The mean wavelength ($\bar{\lambda}$) was obtained from the absorption cross section data using equation [30] .

$$\bar{\lambda} = \frac{\sum \sigma(\lambda)}{\sum \lambda\sigma(\lambda)} \qquad (1)$$

Transitions of ions in the glass are mainly due to the presence of magnetic and electric dipoles. The transitions of magnetic dipoles occur between similar parity states, whereas the transitionsof electric dipoles occur between the states of odd parity.Theradiativetransitionsleading to absorption spectra takes place due to the transition from higherexcitedstatesto lowerlyingstatesA(J'→J). The radiative transition probabilities,$A(\Psi_J, \Psi'^{J'})$, of all the excited states were calculated using equation [34].

$$A_R(\Psi_J, \Psi'^{J'}) = \frac{64\pi^4\tilde{\nu}^3}{3h(2J+1)}\left[\frac{n(n^2+2)^2}{9} S_{ED} + n^3 S_{MD}\right] \qquad (2)$$

Where, n is the refractive index of glass, S_{ED} and S_{MD} are the electric and magnetic dipole line strengths respectively. J is the total angular momentum quantum number of higher excited state. The line strengths of electric dipole transitions and magnetic dipole transitions were calculated using equations (3) and (4) respectively [30].

$$S_{ED} = \sum_{\lambda=2,4,6} \Omega_\lambda \left|\left\{(S,L)J\right\|U^{(\lambda)}\left\|(S',L')J'\right\}\right|^2 \qquad (3)$$

$$S_{MD} = \frac{e^2h^2}{16\pi^2mc^2}\left|\left\{(S,L)J\right\|L+2S\left\|(S',L')J'\right\}\right|^2 (4)$$

The magnetic dipole transitions are non-zero, only if S = S' and L = L'. Additional selection rules for total angular momentum are$J = J'$, $J = (J' + 1)$, $J = (J' - 1)$. The estimation ofmagneticdipole moment using the matrixelementsinLScouplingschemesaresimple and canbe determinedfrom the equation (5), which is derived from the concept of angular momentum [35]. The line strength as predicted by the Judd-Ofelt theory is given by equation (5) [31,32].

$$S_{cal}(J \to J') = \sum_{\lambda=2,4,6} \Omega_\lambda \left|\left\{(S,L)J\right\|U^{(\lambda)}\left\|(S',L')J'\right\}\right|^2 \qquad (5)$$

Where,$||U^{(\lambda)}||$ are doubly reduced unit tensor operators taken from the reference [33], and were tabulated in Table 1. The method of least square fit was employed to determine the Judd-Ofelt intensity parameters using the measured values and predicted values of line strengths. The calculated JO intensity parameters for the entire sample were tabulated in Table 2. (for LBE5 glass).

The Judd-Ofelt intensity parameters ($\Omega_\lambda(\lambda = 2, 4 \,\&\, 6)$) and spectroscopic quality factor ($\chi = \Omega_4/\Omega_6$)confirms that it the glass prepared in the present study can become a good material for the laser production [36].The Judd-Ofelt theory was applied to 0.5 mol % of Er^{3+}doped glass system. The Judd-Ofelt intensity parameter relates the distinct collection and bonding conditions of the RE^{3+} ions. These parameter show not only covalence of bonds but also on the irregularity of vicinity of the RE^{3+} ions. The estimated JO intensity parameters ($\Omega_{2,4,6}$) and spectroscopic quality factor of the glasses were shown in the Table 2. Usually the magnitudes of Ω_2 parameter depends on the asymmetric and covalence type among ions and rare-earth ions [35], while other values of $\Omega_4$and Ω_6 depend on viscosity and rigidity of the host medium. The measured values of three JO intensity parameters of the LBE glasseswere in the order $\Omega_2 > \Omega_6 > \Omega_4$as shown Table 2. The values of intensity parameters obtained shows that the Er^{3+}ions are established in a higher covalence situation within the glass network.

Themeasuredradiativetransitionrates(A_{MD} and A_{ED})weregivenin the Table 3. The total radiative transition probability (A_T)is given by

$$A_T = \sum_{J'} A\left(\Psi_J, \Psi'^{J'}\right) \qquad (6)$$

The branching ratio describes the interaction of light and ions as a function of wavelength of allowed transition to an excited state, which is determined using the equation (7) [37].

$$\beta_{cal}\left(\Psi_J, \Psi'^{J'}\right) = \frac{A_R\left(\Psi_J, \Psi'^{J'}\right)}{A_T} \qquad (7)$$

The measurement of radiative life times isquite difficult, hence, it is indirectly calculated in most of the cases. The difficulty is due to existence of spontaneous emission.Also, it includes energy transfer, non-radiative relaxation and radiative trapping. As a result, directly measurement ofthe life time does not yield radiative lifetime at any temperature. Therefore, utilizing the reciprocal of the absorption indeed, the radiative lifetime can be calculated using the equation (8) [37].

$$\tau_{rad} = \frac{1}{\sum A_T(J \to J')} \qquad (8)$$

The emission cross section depends on the composition of the glasses. By taking into the consideration of relation between radiative transition, branching ratio and refractive index, the emission cross section can be calculated using the equation [37].

$$\sigma = \frac{\lambda^2 \beta_{rad}(J \to J')}{8\pi c n^2 \tau_{rad}} g(\bar{\nu}) \qquad (9)$$

The radiative transition probabilities are present in the LBE glasses is in good agreement with the reported values [38]. Therefore, these glasses can be treated as host materials for broad band amplifier [39,40] The line shape function, $g(\bar{\nu})$ is given by [37].

$$g(\bar{\nu}) = \frac{I(\bar{\nu})}{\int I(\bar{\nu})\, d\bar{\nu}} \qquad (10)$$

The figure of merit (FOM) for optical gain, given by($\sigma_e \times \Delta\lambda_{eff}$), shows the band width of an amplifier. The FOM values in Table 4 match with other Er^{3+}doped glasses are good host materials for the broad band amplifiers. Corresponding to each transition we have also estimated band width gain ($\sigma_e \times \Delta\lambda_{eff}$). The values of S_{ED}, A_{ED}, A_{MD}, A_T, β_{meas}, $g(\bar{\nu})$, σ are tabulated in Table 3 and 4.

Table 1. Reduced matrix elements for absorption peaks of Er^{3+} ion used in the calculations

Transition	U(2)	U(4)	U(6)	RME(MD)
$^4G_{7/2}$-$^4I_{15/2}$	0	0.0334	0.0029	0.00000
$^4G_{5/2}$-$^4I_{15/2}$	0	0	0.0026	0.00000
$^2P_{3/2}$-$^4I_{15/2}$	0	0	0.0172	0.00000
$^2G_{7/2}$-$^4I_{15/2}$	0	0.017411	0.116315	0.00000
$^2K_{15/2}$-$^4I_{15/2}$	0.021974	0.004095	0.075754	0.53157
$^4G_{11/2}$-$^4I_{15/2}$	0.918357	0.526087	0.117176	0.000000
$^2G_{9/2}$-$^4I_{15/2}$	0	0.01896	0.225554	0.000000
$^4F_{3/2}$-$^4I_{15/2}$	0	0	0.1272	0.000000
$^4F_{5/2}$-$^4I_{15/2}$	0	0	0.22321	0.000000
$^4F_{7/2}$-$^4I_{15/2}$	0	0.146878	0.626538	0.000000
$^2H_{11/2}$-$^4I_{15/2}$	0.712554	0.412365	0.092467	0.000000
$^4F_{9/2}$-$^4I_{15/2}$	0	0.535386	0.461795	0.000000

Table 2: JO intensity parameters (in 10^{-20}cm^2 units) and spectroscopic quality (χ) for the Er^{3+} doped other glasses.

Glass	Ω_2	Ω_4	Ω_6	χ	Reference
NfBEr	1.125	0.646	0.366	1.76	[79]
Bismuthate	3.86	1.52	1.17	1.11	[73]
Sodalime silicate	2.72	2.31	1.28	1.8	[74]
Tellurite	5.22	1.55	1.13	1.371	[56]
Borosilicate	4.13	1.83	1.63	1.123	[75]
Lithium borate	3.24	0.92	0.82	1.123	[76]
ZBE3	3.02	1.32	1.22	1.082	[26]
Phospate	5.0	1.5	1.07	1.402	[78]
LBE5	O.1698	0.0816	0.0903	0.9035	Present work

Table 3: Line strengths ($\times 10^{-20} cm^2$), transition probabilities, branching ratios.

Transition	λ(nm)	S_{ED} (calculated)	S_{ED} (measured)	$A_{ED}s^{-1}$	$A_{MD}s^{-1}$	β
$^4G_{7/2}$-$^4I_{15/2}$	293	0.029018	0.0206	15.605	0.000	0.0035
$^4G_{5/2}$-$^4I_{15/2}$	301	0.045969	0.0000	0.008	0.000	0.0000
$^2P_{3/2}$-$^4I_{15/2}$	314	0.015570	0.0238	12.806	0.000	0.0006

$^2G_{7/2}$-$^4I_{15/2}$	355	0.041973	0.0309	5.741	0.000	0.0020
$^2K_{15/2}$-$^4I_{15/2}$	364	0.051619	0.0154	1.325	0.010	0.0032
$^4G_{11/2}$-$^4I_{15/2}$	377	0.0018929	0.0262	2.712	0.201	0.0124
$^2G_{9/2}$-$^4I_{15/2}$	406	0.0246012	0.0219	2.177	0.000	0.0183
$^4F_{3/2}$-$^4I_{15/2}$	441	0.040286	0.0057	1.046	0.000	0.0073
$^4F_{5/2}$-$^4I_{15/2}$	450	0.038282	0.0115	1.395	0.000	0.1768
$^4F_{7/2}$-$^4I_{15/2}$	488	0.044015	0.0017	0.122	0.150	0.0388
$^2H_{11/2}$-$^4I_{15/2}$	520	0.0018781	0.0157	0.618	0.000	0.1432
$^4F_{9/2}$-$^4I_{15/2}$	651	0.090967	0.0082	486.902	0.0000	1.000

Table 4: Calculated total transition probabilities, line shape functions, emission cross sections ($\times 10^{-22} cm^2$), optical gain($\times 10^{-25} cm^2 s$), and gain bandwidth ($\times 10^{-28} cm^3$).

Transition	$A_T s^{-1}$	$E\ cm^{-}$	Lifetime (ms)	$g(\bar{\nu})$	σ	Optical Gain	Gain Bandwidth
$^4G_{7/2}$-$^4I_{15/2}$	15.605	34130	0.2245	0.128276	4.2583	0.95599	3.31967
$^4G_{5/2}$-$^4I_{15/2}$	0.008	33223	0.5751	0.079034	0	0	0
$^2P_{3/2}$-$^4I_{15/2}$	12.806	31847	0.0451	0.221208	7.1969	0.32458	3.25343
$^2G_{7/2}$-$^4I_{15/2}$	5.741	28169	0.3536	0.147323	2.6047	0.921013	1.768
$^2K_{15/2}$-$^4I_{15/2}$	1.335	27473	2.4228	0.137324	0.59606	1.44413	0.434053
$^4G_{11/2}$-$^4I_{15/2}$	2.913	26525	4.2500	0.153202	1.5758	6.69695	1.02855
$^2G_{9/2}$-$^4I_{15/2}$	2.177	24631	8.4098	0.117907	1.04897	8.82164	0.889663
$^4F_{3/2}$-$^4I_{15/2}$	1.046	22676	7.0239	0.062368	0.31267	2.19617	0.501337
$^4F_{5/2}$-$^4I_{15/2}$	1.395	22222	126.769	0.072953	0.51103	64.7823	0.70049
$^4F_{7/2}$-$^4I_{15/2}$	0.272	20492	142.208	0.076586	0.123425	17.5521	0.161159
$^2H_{11/2}$-$^4I_{15/2}$	0.618	19231	231.804	0.080302	0.33271	77.123	0.41432
$^4F_{9/2}$-$^4I_{15/2}$	486.902	15361	2.0538	0.040292	206.222	423.54	511.813

3.2 Photoluminescence studies

The excitation spectra of Er^{3+}doped LBE borate glasses showed intense peaks at 397 nm which corresponds to the electronic transition of $^4I_{15/2} \rightarrow {}^4G_{11/2}$as shown in the Fig 3a. The glass system showedpeak emission spectrum at 545 nm of the LBE glasses in the wavelength range of 380 – 650 nm. The transitions from ground state to the excited states prounced at 369, 397, 437, 449, 446, 479 and 494 nm, shown in Fig 3b, corresponding to $^4I_{15/2} \rightarrow {}^4G_{9/2}$, $^4G_{11/2}$, $^4H_{9/2}$, $^4F_{3/2}{}^4F_{5/2}$, $^4F_{7/2}$transitions respectively [41]. By observing these transitions, electronic transition $^4I_{15/2} \rightarrow {}^4G_{11/2}$is assigned to the wavelength 397 nm is observing the maximum intensity and same has been chosen as an excitation spectrum of LBE glasses. The obtained emission spectrum shows four pertinent peaks at 440 nm, 494 nm, 529 nm and 545 nm corresponding to the electronic transitions from$^4F_{5/2}{}^4F_{7/2}$, $^2H_{11/2}$and $^2S_{3/2}$to the ground state $^4I_{15/2}$ of Er^{3+}ions respectively as shown in the Fig 3a. The Er^{3+}ion goes to the excited state $^4G_{11/2}$ by absorbing the wavelength of 397 nm. In this excitation, the emission of band blue (between range of 474 to 481 nm), green band (between range of 510 to 580 nm) and red band (between range of 640 to 645 nm) [42]. These bands arise due to emission from the excited from higher energy state from ground state absorption and excited state absorption in the Er^{3+}energy states. We confirm that investigated glasses contain basic colors of green, red, and blue emissions. These color combinations could lead to the obtain the white color emission from the glass which clearly confirm from the CIE color coordinate analysis explained in the proceedings section. In the way to identify the color of the emitted light, the investigation in the color emitted by the source by comparing with the standard color emitted by the white light emitting source.

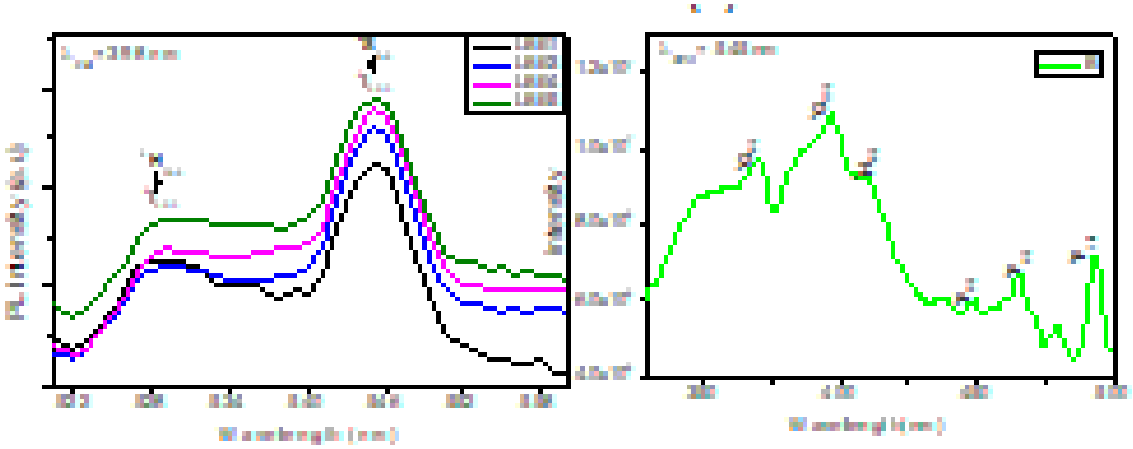


Fig 3a. Visible-Photoluminescence spectra of LBE glasses of Excited wavelength 398nm.

Fig 3b.Visible-Photoluminescence emission spectra of wavelength 545nm.

3.3 Photometric analysis (CIE & CCT)

The emission of white light in the Er^{3+}doped bismuth-borate glass has been confirmed in the commission international deI'Echairage (CIE) 1931chromaticity as shown in the Fig 3b. The CIE chromaticity diagram for different mol % of Er^{3+}doped glasses are obtained from the florescence emission spectra in the visible region under the excitation wavelength of 397nm. The CIE chromaticity coordinates and corresponding correlated color temperature values of different concentration of Er^{3+}doped glasses were listed in the Table 5. Under CIE chromaticity diagram we have noticed that, the emission fluorescence spectra exhibit white light in the visible region. The estimated LBE glass spectra under excitation of 397nm which are close to the expectedvalue of the white light coordinates (0.333, 0.333). This confirms that, highest doped Er^{3+} (LBE5) glass sample can exhibit

better fluorescence compared to the other samples.

The correlated color temperature (CCT) values were obtained from the CIE chromaticity diagram coordinates by using the McCamy's approximate formula [43]. $CCT = -449n^3 + 3525n^2 - 6823.3n + 5520.33$. where $n = \frac{X-X_e}{Y-Y_e}$ and$(X_e = 0.332, Y_e = 0.186)$ is the epic center of the merging. The estimated CCT value for Er^{3+}doped glasses is 10784k ,which is close to white light zone in the chromaticity order as shown in the Fig 3b. It can be noted that, as CCT values are higher, the perception of brightness is good with an improved usual perception [44].

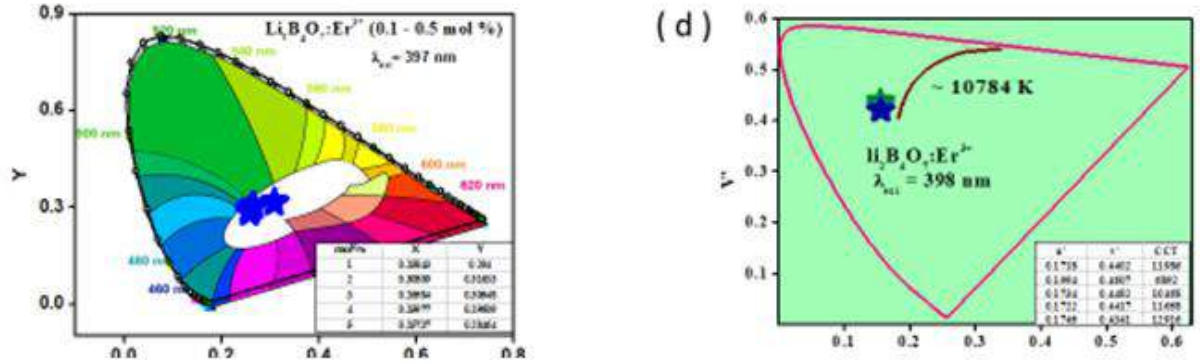


Fig 4a. CIE chromaticity of coordinates for Er^{3+} doped LBE glasses under excitation wavelength 398nm.and Fig 4b. CCT coordinates of 0.1, 0.2, 0.3, 0.4, and 0.5 mol% of Er^{3+} doped LBE glasses.

Table 5.CIE chromacity coordinates and CCT value Er^{3+} doped LBE glasses under excitation wavelength of 398nm.

No	Glass composition	CIE chromacity (x, y)	CCT
1	Li_2O-B_2O_3-$BiCl_3$; Er^{3+} (0.1mol%)	(0.25824, 0.294)	11986
2	Li_2O-B_2O_3-$BiCl_3$; Er^{3+} (0.2mol%)	(0.30809, 0.31633)	6892
3	Li_2O-B_2O_3-$BiCl_3$; Er^{3+} (0.3mol%)	(0.26584, 0.30548)	10468
4	Li_2O-B_2O_3-$BiCl_3$; Er^{3+} (0.4mol%)	(0.25977, 0.29609)	11658
5	Li_2O-B_2O_3-$BiCl_3$; Er^{3+} (0.5mol%)	(0.25737, 0.28464)	12916

4. CONCLUSION

The absorption spectra of Er^{3+} doped LBE glasses possess very sensitive spectroscopic properties have been calculated. Using absorption spectra, the Judd-Ofelt parameter of the glass sample have been calculated. These have been used to calculate to calculate other parameter like oscillatory strength, transition probabilities, radiative life time, and stimulate cross section by using respective relation. It leads tothe better significance of Ω_2 parameter specify that the greater asymmetric environment of the ions site and established through the less ionic character of the Er^{3+} ions with neighboring ligands. The Er^{3+} doped bismuth-borate glasses are also good compared to other borate glasses and some other parameter spectroscopic parameter used in the field of laser technology. The obtained and measured value of the stimulated emission cross section is small discrepancy was observed. The re-emission of Er^{3+} ions of all prepared glass have band width gain, figure of merit (FOM) for LBE glasses and suitable for broad band amplifiers.

REFERENCES

[1]. ShriyaSinha, Manoj Kumar Mahata, Kaushal Kumar, RSC. Adv 6 (2016) 89642-89654.
[2]. Y. C. Lin, M. Karlson, M. Bettinelli. Inorganic Phosphor materils for lighting, Top. Curr. Chem,. 374 (2016) 374-421.
[3]. D. Ramachari, D. Esparza, T. Lopez-luke, V.H. Romero, L. Perez-Mayen, et al., J. Alloys Comp. 698 (2017) 433-441.
[4]. Hao Dong, Ling-Dong Sun, Chun-Hua, Chem. Soc. Rev. 44 (2015) 1608-1634.
[5]. G.A. Kumar, M. Pokhel, D.K. Sardar, Mater. Lett 98 (2013) 63-66.
[6]. T. Li, C. Guo, H. Jiao, L. Li, D.K. Agarwal, Opt. Cummun. 312 (2014) 284.
[7]. K. Annapoorani, Ch. Basavapoornima, N. Suriya Murthy, K. Marimuthu, J. Non-Crys. Solids 447 (2016) 273-282.
[8]. J. A. Caired, A. J. Ramponi, P.R. Staver, J. Opt. Soc. America B, 8 (1991) 1391-1403.
[9]. P. Babu, C.K. jayashankar, opt. Mater. 15 (2000) 65-79.
[10]. Xiang Shen, Quinhua, T. Xu, S. Dai, X. Wang, Physica B, 381 (2006) 219-223.
[11]. K.J. Rao, Structural chemistry of glasses. Elsevier, North Holland (2002).
[12]. G. Chandrashekaraiah, N. Shivashankara Reddy, B. Sujatha, R. Viswanatha, C. Nararaya Reddy. J. Non-Cry. Solids. 498 (2018) 252-261.
[13]. S. Tanable, N. Sigimoto, S. Ito, T. Hanada, J. Lumin. 87-89 (2000) 670-672]
[14]. M. Laya, Krishnan, M.M Neethish, V. V. Ravikanthkumar. J. Lumin. 201 (2008) 442-450.
[15]. F. Ahmadi, R. Hussin, S.K. Ghoshal, J. Alloys Comp. 711 (2017) 94-102.
[16]. Anita Hastir, NipinKohli, Ravi Chand Singh, J. Phys. Chem. Solids 105 (2017) 23-34.
[17]. M. Goppert-Mayer, Ann. Phys.(Berlin) 18 (2009) 466-479.
[18]. W. Kaiser and C.G.B. Garrett, Phys. Rev. Lett. 7(6), (1961) 229-231.
[19]. Foud El-Diasty, F. A. Abdel Wahab, M. Abdel-Baki, J. Appl. Phys. 100, 093511 (2006).
[20]. Reni Iordanova, Margarita, Milonova, LyubomirAleksandrov, AtulKhanna, J. Non-cryst Solids 481 (2018) 254-259.
[21]. P. J. Bray, J. O'Keefe PCG 4 (1963) 37
[22]. E. I. Kamitsos, A. P. Patsis. K. A. karakassides, G.D. chryssikos, J. Non-cryst. Solids, 126 (1990) 52-67.
[23]. E.I. Kamitsos, G.D. Chryssikos. J. MolStruc 247 (1991) 1-16.
[24]. E.I. kamitsos, J. Ephysique IV2 (1992) C2-87).
[25]. P. Babu, H.J. Seo, C.R. Kesavulu, K.H.Jang. C. K. Jayashankar. J. Lumin. 129 (2009) 444-448.
[26]. K. Annapoorni, N. Suriya Murthy, T.R. Ravindran. K. Marimuthu. J. Lumin 171 (2016) 19-26.
[27]. K. Lingaraju, K. Suresh, S. Ju, W-T. Han, et al., Opt. Mater. Express 5 (2015) 1689-1703.
[28]. Ofelt G.S. intensities of crystal spectra of rare-earth ions, J. Chem. Phys. 37 (1962) 511-520..
[29]. Arul Rayappan , k. Marimuthu, J. Phys and Chem. Solids 74 (2013) 1570-1577.
[30]. B.M. Walsh. NASA Langley Research center Hampton, VA 23681 USA.
[31]. Judd, B.R (1962) Optical absorption intensities of rare-earth ions, Phys. 127 (1962) 750-761.
[32]. Ofelt G.S. (1962) intensities of crystal spectra of rare-earth ions, J. Chem. Phys. 37 (1962) 511-520.
[33]. S. Tanabe, X.Feng, T. Hanada, Opt.Lett.25 (2000) 817-819.
[34]. B.M. Walsh, Judd-Ofelt Theory: Principles and Practices in Advances in Spectroscopy for Lasers and Sensing, ed. B. Di Bartolo and O. Forte (Springer, Netherlands, 2006) 403-433.

[35]. B. R. Judd, Operator Techniques in Atomic Spectroscopy (McGraw–Hill, New York, 1963.
[36]. K. Selvaraju, K. Marimutu, Physica B 407 (2012) 1086-1093.
[37]. Dhiraj K. Sardar, Douglas M. Dee, Kelly L. Nash, Raylon M. Yow, and John B. Gruber, Optical absorption intensity analysis and emission cross sections for the intermanifold and the inter-Stark transitions of Nd3+, 4f3+ in polycrystalline ceramic Y 2O 3, J. Appl. Phys. 100 (2006) 123106.
[38]. X. Zou, T. Izumiysni. J. Non-crys. Solids 162 (1993) 68-80.
[39]. R.Rolli, M. Mountaga, S. Chaussedent, A. Monteil, V.K. Tikhomitrov, M. Ferrari, Opt. Mater. 21 (2003) 743-748.
[40]. L.R.P. Kassab, L.C. Courrol, R. Seragioli, N.U. Wetter, S.H. Tatmi, L. Gomes, J. Non-ctyst. Solids. 348 (2004) 94-97.
[41]. L. Vijayalakshmi, K. Naveen Kumar, K. SrinivasaRao, Pyung Hwang, J. Mol. Struc. 1155 (2018) 394-402.
[42]. Anurag Pandey, S. Soma, Vijay Kumar, Vinod Kumar, Kaushal Kumar, Vineet Kumar, H. C. Swart. J. Sensor and Actuators B 202 (2004) 1305-1312.
[43]. Remya Mohan P, Ramya, Subash, Gopi, VijiVidhyadharam, Anns George, Cyriac Joseph, N.V. Unnikrishnan, P.R,.Bijju, J. Lumin. 187 (2017) 113-120.
[44]. Lakshmi Mukhopadhyay, Vineet Kumar Rai, RenukaBakalia, K. Sreenivas, J. Lumin, 187 (2017) 368-377.